Electronic Supplementary Material (ESI) for Photochemical & Photobiological Sciences.

Progressive Cationic Functionalization of Chlorin Derivatives for Antimicrobial Photodynamic Inactivation and Related Vancomycin Conjugate

Liyi Huang,[‡,§] Min Wang,[†] Ying-Ying Huang,[‡,§] Ahmed El-Hussein,[‡,§] Lawrence Wolf,[†] Long Y. Chiang,*[,†] and Michael R. Hamblin*[,‡,§,¥]

[‡] Wellman Center for Photomedicine, Massachusetts General Hospital, Boston, Massachusetts 02114, United States

[§] Department of Dermatology, Harvard Medical School, Boston, Massachusetts 02115, United States

[†] Department of Chemistry, University of Massachusetts Lowell, Lowell, Massachusetts 01854, United States

[¥] Harvard-MIT Division of Health Sciences and Technology, Cambridge, Massachusetts 02139, United States

Supplementary Material

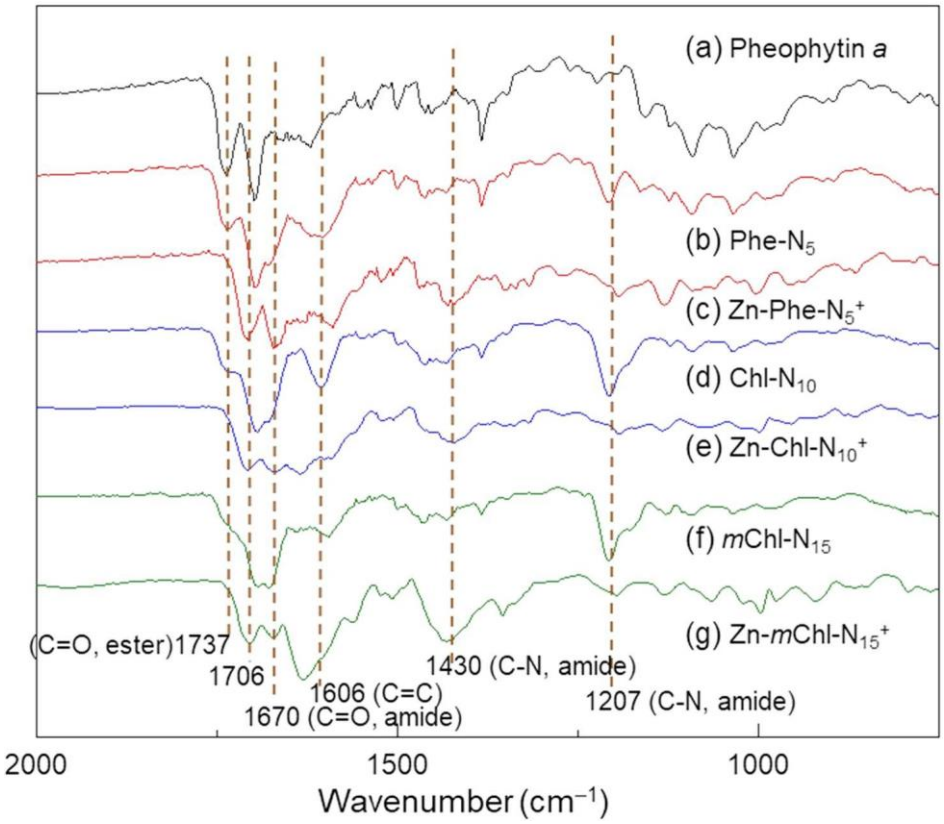

Figure S1. Infrared spectra of four pheophytin and chlorin derivatives as indicated.

Various spectroscopic methods were applied for the characterization of all compounds with the corresponding data included in the experimental section. Since all methyl, ethyl side groups, and ring protons of Zn-Phe-N_5^+, Zn-Chl-N_{10}^+, and Zn-mChl-N_{15}^+ remained identical to those of the parent pheophytin core, therefore, all spectroscopic analyses were based on the comparison with the precursor compound to match with the consistent functional group changes. Accordingly, progressive changes of three infrared absorption bands (Figure S1) of these three compounds at 1670 [–C(=O)-NH–], 1606 (–C=C–), and 1430/1207 [–C(=O)-(N–H)–] cm^{-1} were evaluated as

the indicator of structural modification. Intensity increases of the former band going from pheophytin (Figure S1a) to Phe-N_5 (Figure S1b) and Zn-Phe-N_5^+ (one amide arm, Figure S1c), Chl-N_{10} (Figure S1d) and Zn-Chl-N_{10}^+ (two amide arms, Figure S1e), and then mChl-N_{15} (Figure S1f) and Zn-mChl-N_{15}^+ (three amide arms, Figure S1g) were apparently consistent with an increase

of pentacationic N_5^+-amide arm(s). Similar phenomena were also detected on the latter 1430/1207- band as the absorption of amide C-N functional groups.

In the case of ^{1}H NMR spectroscopic analyses, the number of N,N',N,N,N,N-hexapropyl-penta(aminoethyl)amide (N_5-amide) arms attached on either Phe or chlorin core can be accounted for easily by changes of the measured proton integration ratio in the spectrum. We selected the integration of H_δ located on C_δ or H_β on C_β of either the Phe or chlorin core at δ 8.61–8.64 or 9.58–
9.60 (Figure S2), respectively, as the reference of one-proton count (1.0). Theoretically, integration of two types of protons of each N_5-amide arm with the chemical shift at δ 2.5–3.25 (–N-CH_2–, aminomethylene protons) and δ 0.65–1.08 (–CH_3, end-group methyl protons) should give proton counts of 32(H) and 18(H), respectively, in a ratio of 1.78. By taking the measured proton counts integrated over two chemical shift ranges at δ 2.5/2.75–3.25/4.0 (certain compound-related shifts occurred) and δ 0.65–1.08 as 47.0 and 23.7 in Figure S2b, 80.4 and 40.1 in Figure S2c, and 109.9 and 53.8, respectively, in Figure S2d as the base, we then deducted all other types of non-N_5-amide associated methyl and methylene protons appearing and overlapping in the same chemical shift regions. It resulted in adjusted values of 31.0 and 17.7 in a ratio of 1.75 for one N_5-amide-armed Phe-N_5, 62.4 and 34.1 in a ratio of 1.83 for two N_5-amide-armed Chl-N_{10}, and 91.9 and 47.8 in a ratio of 1.92 for three N_5-amide-armed mChl-N_{15}. These values corresponded well with a proportional ratio of –N-CH_2–/–CH_3 protons among Phe-N_5, Chl-N_{10}, and mChl-N_{15} giving a roughly good agreement with that (1.78) of the N_5-amide arm. In addition, the total accumulative proton counts integrated also matched well with the number increase of N_5-amide arms from one, two, to three going from the structure of Phe-N_5, Chl-N_{10}, to mChl-N_{15}. These results can be regarded as a good consistency with the structural assignment of these compounds after functional modification from the basic Phe or chlorin core moiety. Subsequent reactions of metal (Zn^{2+}) insertion and quaternary methylation to incorporate water-solubility characteristics should not alter the basic substituent structures on the core.

^{1}H NMR spectrum of macromolecule-like Van-Zn-mPhe-N_5 in DMSO-d_6–$CDCl_3$ (Figure S3c) is rather complex. However, two sharp singlet peaks corresponding to H_α (δ 8.82) and H_β (δ 9.28) protons located on C_α and C_β, respectively, of the mesopheophorbide ring moiety can be seen clearly. The overall spectrum also fitted well with the combined spectra of Phe-N_5 in $CDCl_3$ (Figure S3a,) and vancomycin in D_2O (Figure S3b). By taking the integration ratio of 1.0 as one proton count for either a H of Figure S3b or H_β of the Phe ring in Figures S3a and S3c spectra, the sum of aliphatic protons in both Phe and Van moieties matches with the proton counts of the spectrum of Figure S3c in the region of δ 0.3–1.25 and 1.25–2.0, indicating a Phe/Van moiety ratio

of 1:1 consistent with that in the structure of Van-Zn-mPhe-N_5. Disappearance of olefin protons (H_{3b}) in Figure S3c, as marked by red arrow, is also consistent with the attachment of a Van unit on the vinyl carbon of pheophytin moiety.

To verify the degree of quaternization, we selected the synthesis of mChl-N_{15}^+ as an example. As a result, ^{1}H NMR spectra of neutral mChl-N_{15} (in $CDCl_3$, Figure S4a) and methyl quaternized multicationic mChl-N_{15}^+ (in DMSO-d_6, Figure S4b) showed nearly quantitative conversion using methyl iodide as the quaternization agent. The precursor mChl-N_{15} compound displayed the chemical shift of methylene protons next to tertiary amines at δ 2.5–3.4. Upon quaternization, the chemical shift of these methylene protons down-shifted to δ 3.3–4.3 leaving the region of δ 2.5–3.0 with nearly no proton bands in the spectrum of Figure S4b, marked by red arrow. This is indicative of approximately full chemical conversion to cationic states as mChl-N_{15}^+. Meanwhile, a new sharp singlet peak of methyl protons next to the quaternary amine was detected at δ 3.10.

Furthermore, to increase the spectroscopic detection resolution, we used non-ionic precursor compounds, such as Phe-N_5, Chl-N_{10}, mChl-N_{15}, and Van-mPhe-N_5, instead of multicationic PSs for the verification of their molecular mass after covalent conjugation reactions with different moieties. We detected the corresponding molecular mass ions using the matrix-assisted laser desorption ionization (MALDI-TOF) mass spectroscopy technique, where 3,5-dimethoxy-4- hydroxycinnamic acid was used as the matrix material. As a result, we were able to observe several molecular mass ions at m/z 1059–1061 (MH^+, Figure S5a), 1545 (MH^+, Figure S5b), 2045 (MH^+, Figure S5c), and 2525 (M^+, Figure S5d), respectively, for these four precursor compounds that indicated successful conjugation reactions of both pheophorbide and chlorin-e_6 ring moieties with either pentacationic N_5^+-arm(s) or the vancomycin unit. We propose a fragmentation path having the loss of N_6-arm(s) as the main event in all spectra. Owing to a relatively high molecular weight of Van-mPhe-N_5 and less volatility under MALDI conditions, its spectral resolution at the high mass region of Figure S5d was expected to be less than those of Figures S5a–S5c. However, we were still able to detect its molecular mass ion (MH^+) at m/z 2525. Apparently, the facile loss of vancomycin moiety occurred to give fragmented mass ions at m/z 1120, corresponding to the proposed bond cleavage shown in Figure S6. This substantiated the mPhe–Van conjugation. Low versatility of polycationic Zn-Phe-N_5^+, Zn-Chl-N_{10}^+, Zn-mChl-N_{15}^+, and Zn-Van-mPhe-N_5^+ prohibited their detection by MALDI-TOF mass spectroscopy.

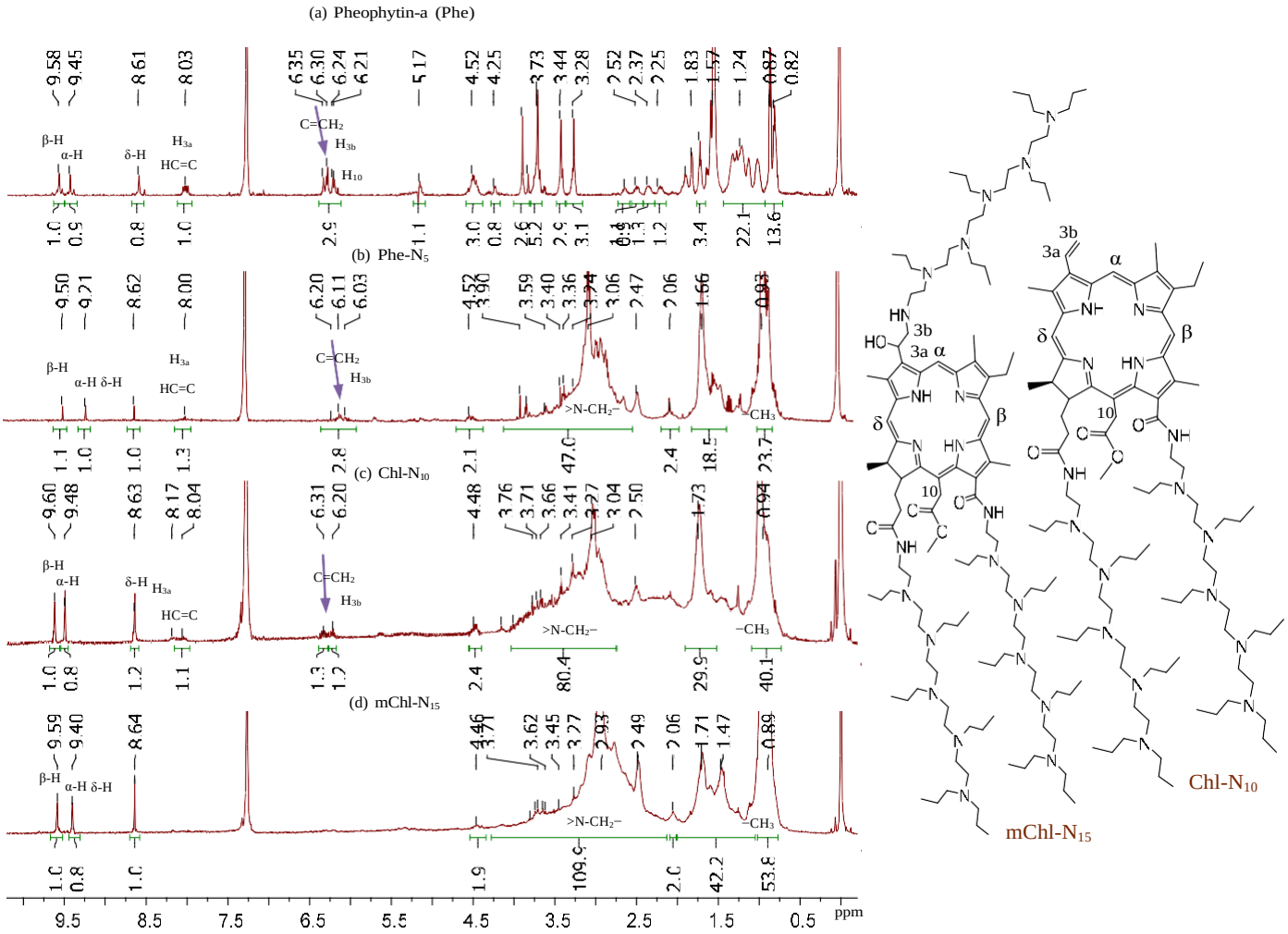

Figure S2. ^{1}H NMR spectra of (a) the starting Phe compound as the reference, (b) Phe-N_5, (c) Chl-N_{10}, and (d) mChl- N_{15}. They all showed the approximate retention in chemical shift value of three pheophytin-a ring protons α-H, β-H, and δ–H at δ 8.5–9.6, as indicated. Disappearance of vinyl proton (H_{3a} and H_{3b}) peaks in the spectrum of (d) centered at δ 8.1 and 6.3, respectively, consisted with one N_6-arm attachment at C_{3b} carbon. The overall proton integration in the region of δ 0.5–4.0 matches well with the corresponding addition of N_6-arm(s) in Phe-N_5 (b), Chl-N_{10} (c), and mChl-N_{15} (d). Finally, metalation of these compounds with Zn to the corresponding Zn-Phe-N_5, Zn-Chl-N_{10}, and Zn-mChl-N_{15} essentially quenched the peak resolution of all spectra.

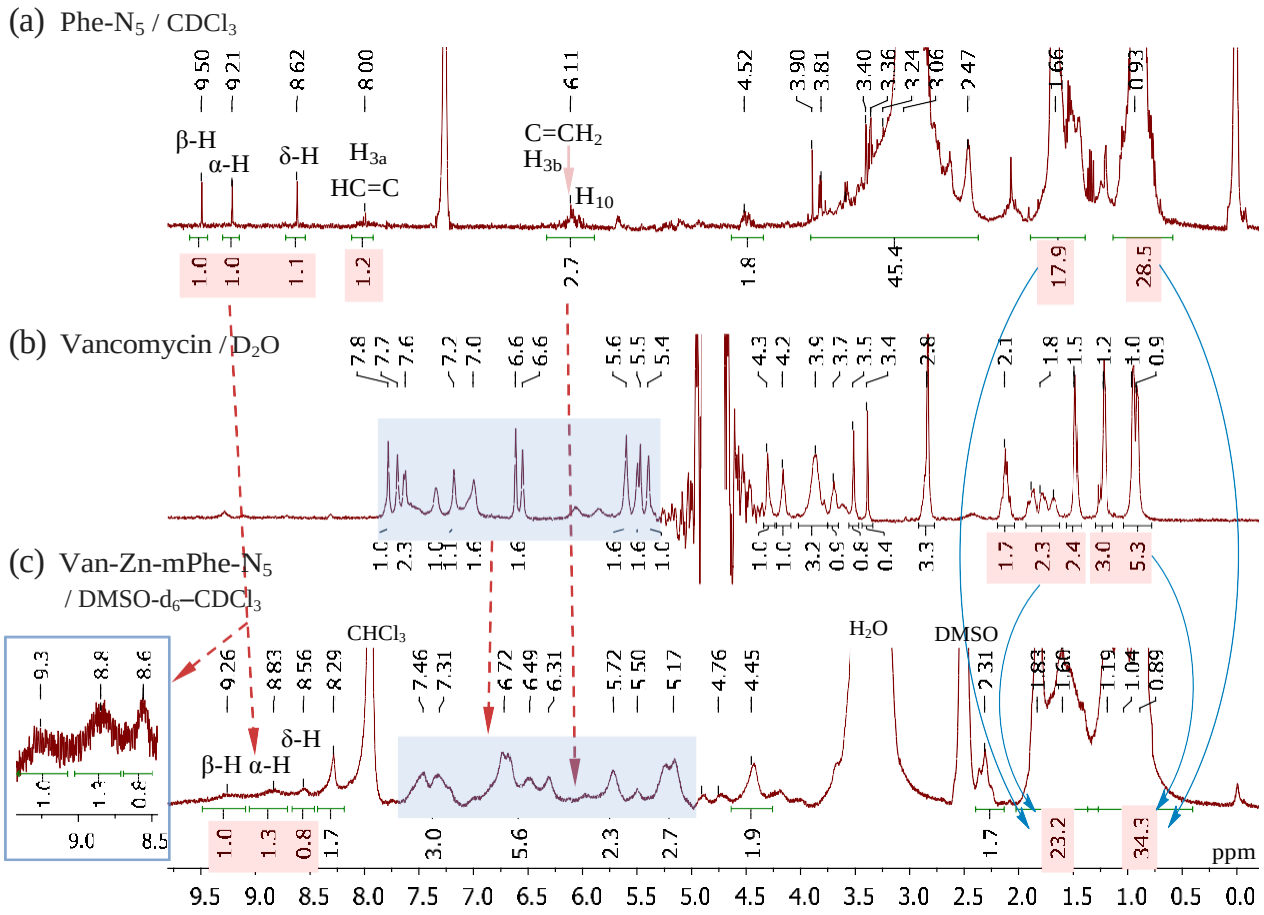

Figure S3. ^{1}HNMR spectra of (a) Phe-N_5 (in $CDCl_3$ for comparison), (b) vancomycin reference (in D_2O), and (c) Van-Zn-mPhe-N_5 (in DMSO-d_6–$CDCl_3$). By taking the integration ratio of 1.0 as one proton count for either a H of (b) or H_β of the pheophytin (Phe) ring in (a) and (c) spectra, the sum of aliphatic protons in both Phe and vancomycin (Van) moieties matches with the proton counts of the spectrum (c) in the region of δ 0.3–1.25 and 1.25–2.0, indicating a Phe/Van moiety ratio of 1:1 consistent with that in the structure of Van-Zn- mPhe-N_5. Disappearance of olefin protons (H_{3b}) in (c), as marked by red arrow, is also consistent with the attachment of a Van unit on the vinyl carbon of pheophytin moiety.

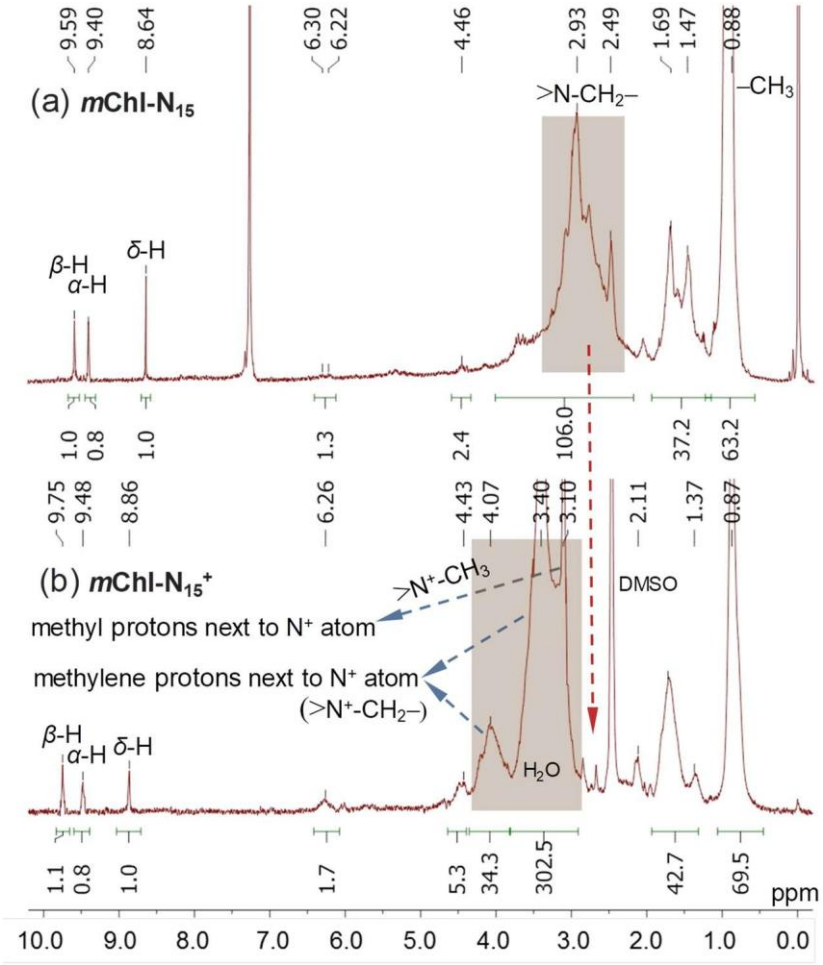

Figure S4. ^{1}H NMR spectra of (a) neutral mChl-N_{15} (in $CDCl_3$) and (b) methyl quaternized mChl-N_{15}^{+} (in DMSO-d_6) to show nearly quantitative conversion using methyl iodide as the quaternization agent, as an example. The precursor neutral mChl-N_{15} compound displayed the chemical shift of methylene protons next to tertiary amines at δ 2.5–3.4 in the spectrum of (a). Upon quaternization, the chemical shift of these methylene protons down-shifted to δ 3.3–4.3 leaving the region of δ 2.5–3.0 with nearly no proton bands in the spectrum of (b), marked by red arrow. This is indicative of approximately full chemical conversion to cationic states as mChl-N_{15}^{+}. Meanwhile, a new sharp singlet peak of methyl protons next to the quaternary amine was detected at δ 3.10.

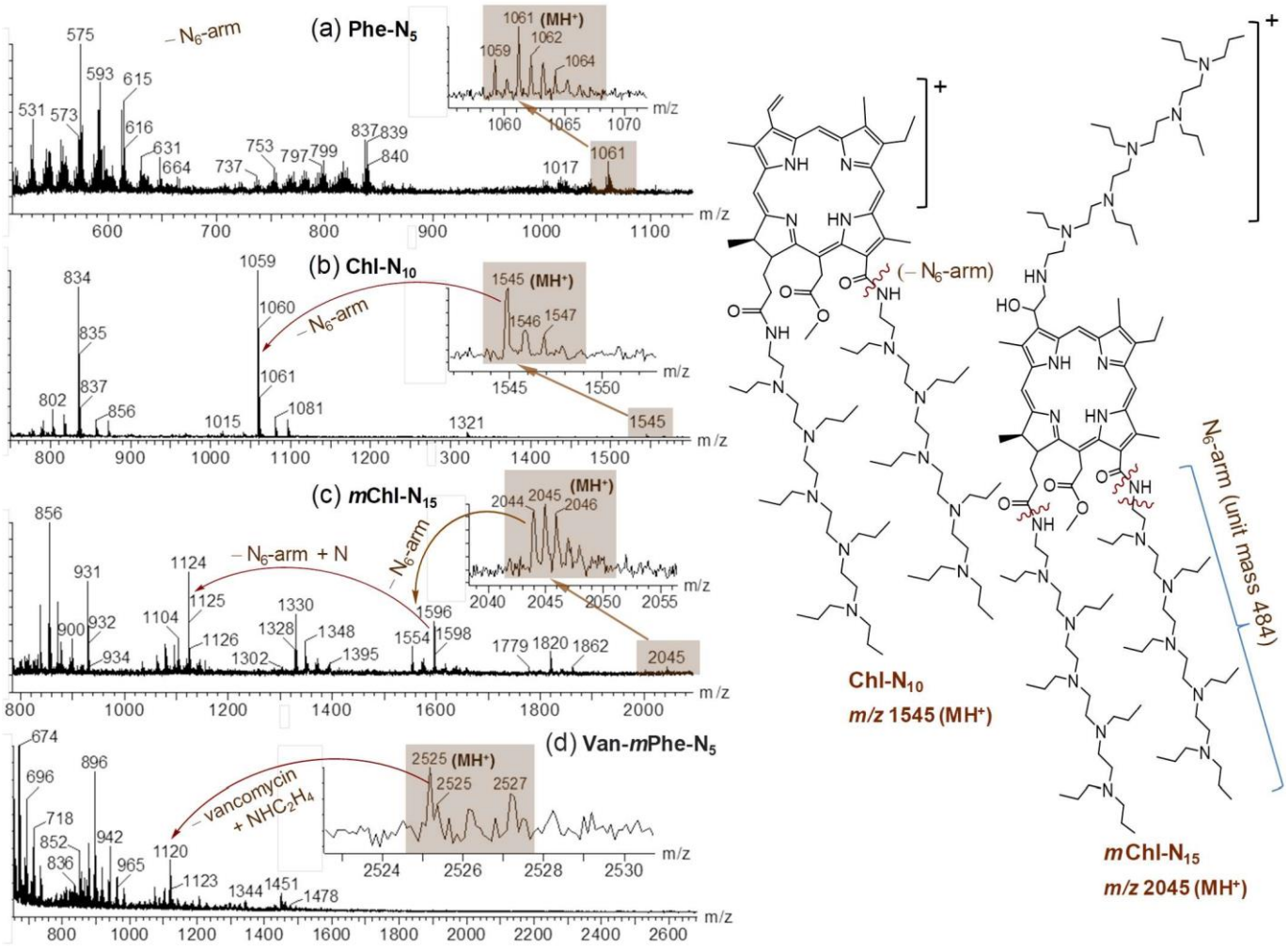

Figure S5. MALDI-TOF mass spectra of (a) Phe-N_5, (b) Chl-N_{10}, (c) mChl-N_{15}, and (d) Van-mPhe-N_5 showing the corresponding molecular mass ions (either M^+ or MH^+), marked by brown shades, with the proposed fragmentation path having the loss of N_6-arm(s) as the main event, as indicated. The data verified the matching molecular weight of these four compounds. Owing to a relatively high molecular weight of Van-mPhe-N_5 and less volatility under MALDI conditions, its spectral resolution at the high mass region of (d) was expected to be less than those of (a)–(c). However, we were still able to detect its molecular mass ion (MH^+) at m/z 2525. Apparently, the facile loss of vancomycin moiety occurred to give fragmented mass ions at m/z 1120, corresponding to the proposed bond cleavage shown in Figure S6. Low versatility of polycationic Zn-Phe-N_5^+, Zn-Chl-N_{10}^+, Zn-mChl-N_{15}^+, and Zn-Van-mPhe-N_5^+ prohibited their detection by MALDI-TOF mass spectroscopy.

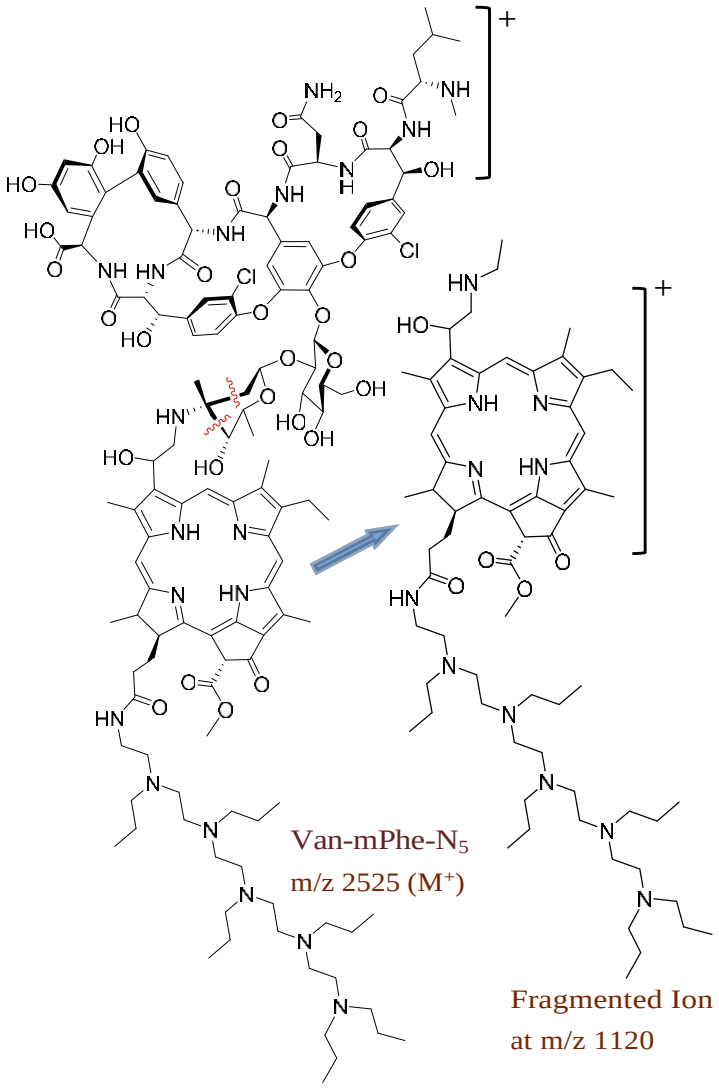

Figure S6. Proposed MALDI-TOF mass fragmentation of Van-mPhe-N_5 showing a group of mass ions centered at m/z 1120 (Figure S4d) with the loss of one (vancomycin mass – NHC_2H_4 mass unit). corresponding to cleavage at two bonds (marked by red) around the hindered, substituted ring carbon center indicated.

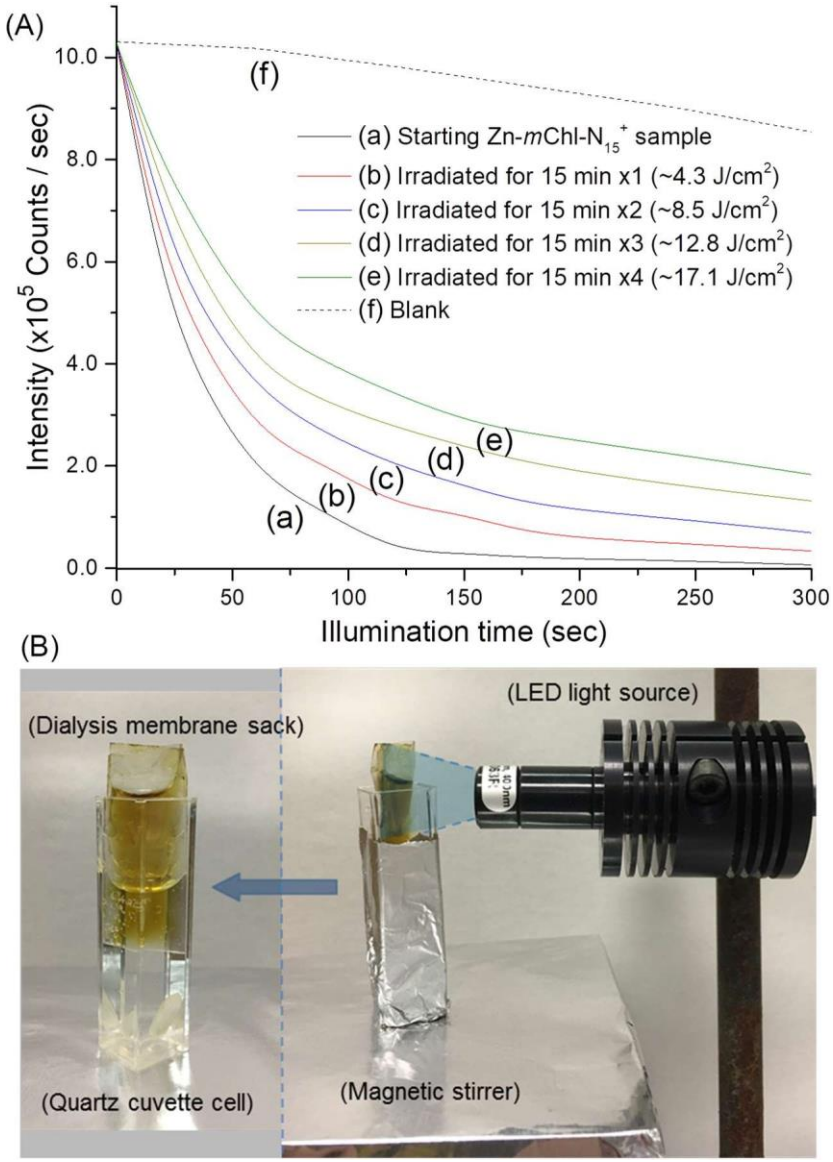

Figure S7. (A) Photostability evaluation of Zn-mChl-N_{15}^+ in D.I, water (5 □ 10^{-6} M) using a singlet oxygen probe ABMA (λ_{ex}350 nm, λ_{em}428 nm) to monitor the $^1O_2$-generation efficiency under irradiation of a white LED light for a period of 15 min once, twice, three times, and four times that accumulated the total light fluence going from 4.3, 8.5, 12.8, to 17.1 J/cm^2, respectively. A progressive slow photodegradation of the sample was observed as the curve slope decreasing from (a) to (e). However, even after a moderate total fluence of photoexcitation at 17.1 J/cm^2 in the similar range of this study, the $^1O_2$-production rate [curve (e)] was still significantly detectable, as compared with the blank [curve (f)]. Assuming the similar photodegradation rate for all samples, owing to the same photosensitizing pheophytin core, the aPDI activity comparison among these samples should be valid. (B) The experimental setup of ROS measurements with fluorescent probes.

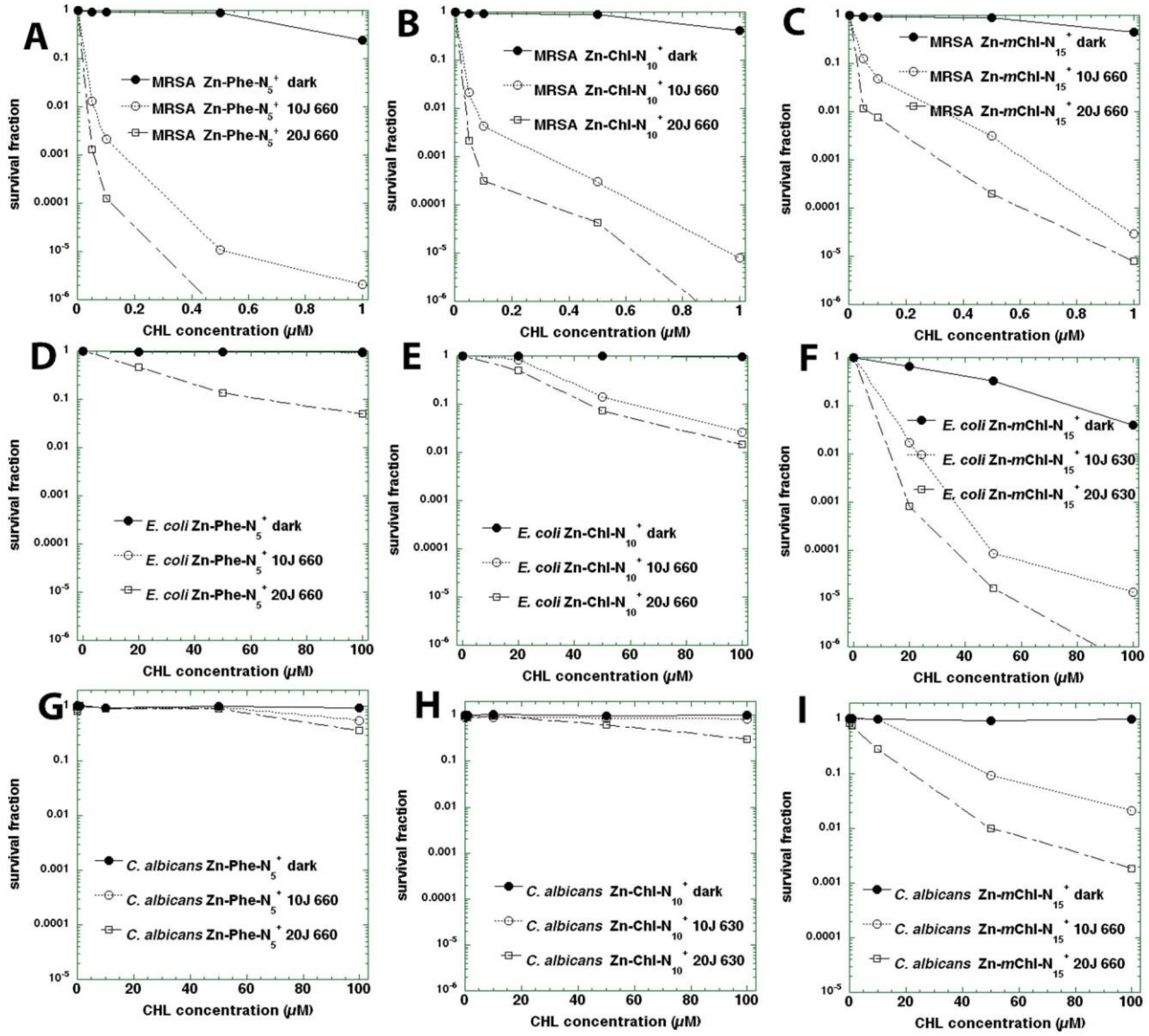

Figure S8. aPDI of Gram-positive MRSA (A–C); Gram-negative E. coli (D–F); fungal yeast C. albicans (G– I). Survival fractions of bacteria (10^8 cells/mL) or fungi (10^7 cells/mL) incubated for 30 min with increasing concentrations of (A, D, G) Zn-Phe-N_5^+, (B, E, H) Zn-Chl-N_{10}^+, or (C, F, I) Zn-mChl-N_{15}^+ followed by illumination with either 10 or 20 J/cm^2 of a 660±15-nm LED light.

The $S_0 \rightarrow S_1$ energy gap is predicted to change very little depending on whether the pendant vinyl group is present (model B), or is saturated (model A), or if an ammonium cation is introduced (model C). Based on the computed geometries, the vinyl group is not completely coplanar with the aromatic π system. The lack of coplanarity reduces conjugation which causes little to no effect on the $\pi \rightarrow \pi^*$ transition.

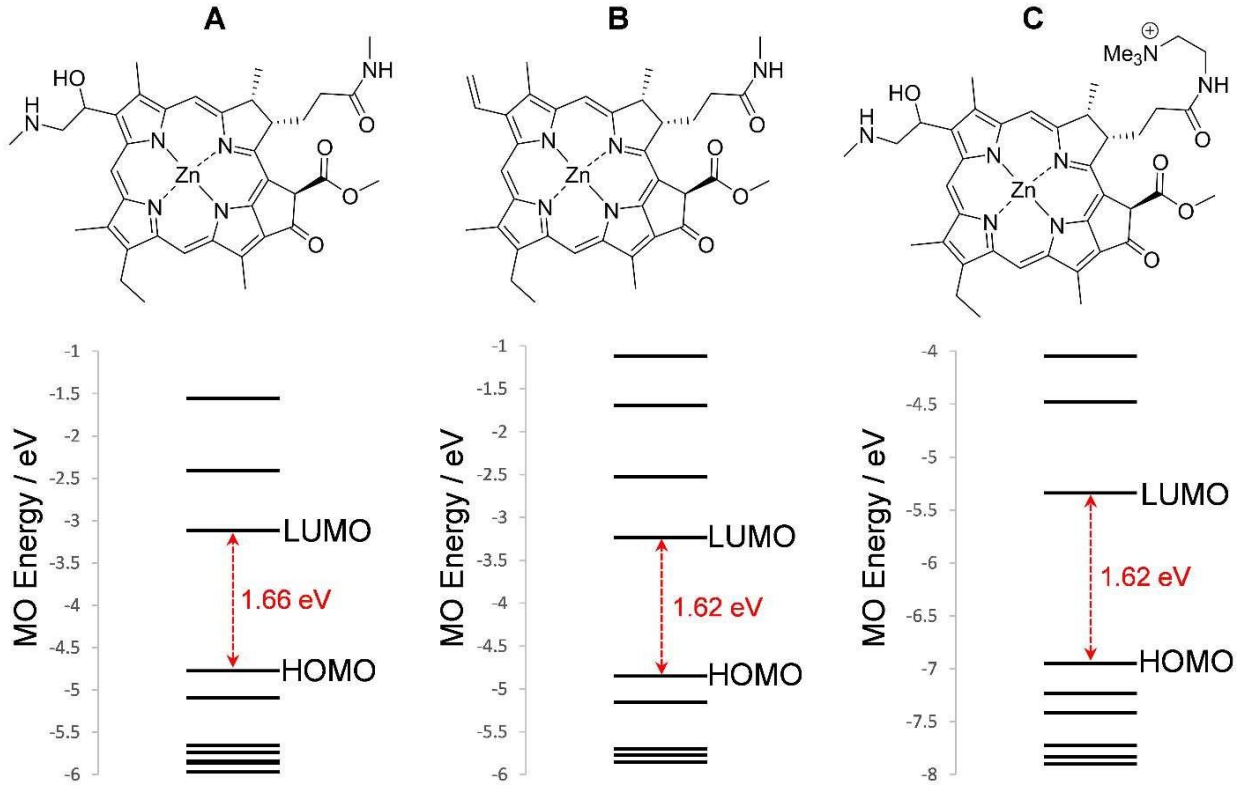

Figure S9. Orbital energy diagrams for the three model systems (A, B, and C) investigated computed at the M06L/def2-TZVPP//M06L/6/31+G(d,p) level of DFT.

Cartesian Coordinates.

A

N	-1.70754	2.22123	-0.03701
C	-3.06728	2.14974	-0.06643
C	-3.64485	3.43752	0.23597
C	-2.59157	4.29732	0.44626
C	-1.38584	3.51996	0.27716
C	-3.78119	0.97511	-0.35261
C	-5.10058	3.73509	0.31180
C	-2.65090	5.73734	0.83527
C	-0.07823	3.99290	0.41582
C	1.09292	3.24687	0.27178
H	0.04009	5.04448	0.67052
N	1.08075	1.89158	-0.05532
C	2.44771	3.71151	0.44207

C	3.24157	2.59219	0.21616
C	2.86359	5.09634	0.78253
C	2.36546	1.52011	-0.08144
C	4.60715	2.09789	0.17557
C	-3.27392	-0.28378	-0.65324
H	-4.86487	1.06811	-0.34544
N	-1.92939	-0.59713	-0.72822
C	-4.05689	-1.46399	-0.94618
C	-3.17198	-2.48308	-1.19999
C	-1.84820	-1.91570	-1.06871
C	-3.43858	-3.90818	-1.53625
C	-0.65983	-2.63045	-1.28224
C	0.64769	-2.18276	-1.17040
H	-0.78558	-3.66614	-1.58717
N	1.01294	-0.93894	-0.77507
C	2.37728	-0.87096	-0.67428
C	3.01545	0.29939	-0.32458
O	5.66677	2.67653	0.34086
C	4.49962	0.55310	-0.12117
H	4.89325	0.02332	0.75530
C	5.37117	0.13555	-1.28082
H	-4.50742	-4.09992	-1.62358
H	-3.01899	-4.58124	-0.77878
H	-2.97738	-4.18497	-2.49138
H	-5.57832	3.22876	1.15961
H	-5.63333	3.41289	-0.59005
H	-5.28279	4.80647	0.43406
H	-3.55257	6.19420	0.40884
H	-1.80822	6.28077	0.38977
C	-2.64827	5.94523	2.34908
H	-3.50916	5.45223	2.81211
H	-2.68803	7.00742	2.60786
H	-1.74791	5.52007	2.80401
H	2.38976	5.44687	1.70627
H	2.58061	5.80559	-0.00380
H	3.94513	5.15770	0.91241
O	6.24434	-0.70458	-1.23752
O	5.03598	0.81285	-2.39866
C	5.80861	0.47713	-3.55620
H	5.43067	1.11035	-4.35669
H	5.68055	-0.57906	-3.80705
H	6.86823	0.67080	-3.37722
C	1.86050	-3.01387	-1.53925
C	3.01974	-2.22198	-0.89125
C	3.54920	-2.81013	0.42426
H	3.86947	-2.14954	-1.58088

H	1.96694	-2.90292	-2.63004
C	1.78687	-4.50154	-1.23848
C	2.56366	-2.72395	1.58784
H	4.48216	-2.29956	0.69284
H	3.81697	-3.86070	0.27064
H	1.62963	-4.71095	-0.17614
H	2.71215	-5.00360	-1.53523
H	0.97302	-4.97420	-1.79556
H	2.47088	-1.68922	1.94294
C	2.93484	-3.67355	2.70754
H	1.55866	-3.01754	1.25322
O	3.20212	-4.85183	2.49222
N	2.92886	-3.13094	3.95925
H	2.70994	-2.15250	4.05759
C	3.22762	-3.90151	5.14296
H	3.44676	-4.91995	4.82088
H	2.37759	-3.92275	5.83224
H	4.09946	-3.50190	5.66994
Zn	-0.42819	0.65426	-0.40887
C	-5.54871	-1.52971	-0.89780
O	-6.04627	-2.31740	-1.96818
H	-5.95419	-0.50385	-0.98843
C	-6.04521	-2.10460	0.43017
H	-5.62523	-3.11162	0.55501
N	-7.49657	-2.22933	0.38353
H	-5.67380	-1.49323	1.27248
H	-6.94268	-2.56687	-1.68819
C	-8.04049	-3.02424	1.47242
H	-7.90903	-1.30127	0.41015
H	-7.67304	-4.05127	1.38597
H	-9.13028	-3.05415	1.40081
H	-7.76898	-2.65667	2.47636

B			
N	2.85808	-0.99775	0.05373
C	4.07956	-0.39596	0.10130
C	5.10858	-1.36737	0.38712
C	4.47441	-2.58182	0.50798
C	3.06569	-2.33297	0.30353
C	4.28011	0.97704	-0.10317
C	6.55922	-1.07107	0.53140
C	5.08434	-3.90149	0.84705
C	2.04843	-3.28972	0.35852
C	0.68346	-3.05758	0.18298
H	2.34787	-4.31485	0.56822
N	0.17053	-1.79113	-0.09168

C	-0.38274	-4.02664	0.26476
C	-1.54570	-3.29907	0.03960
C	-0.22758	-5.47982	0.53006
C	-1.15484	-1.95395	-0.17125
C	-2.99347	-3.37983	-0.05681
C	3.32607	1.94917	-0.38113
H	5.31063	1.31863	-0.04492
N	1.97332	1.71968	-0.51879
C	3.60194	3.35583	-0.60239
C	2.38576	3.95948	-0.86838
C	4.91852	3.94943	-0.51457
C	1.39010	2.92032	-0.81722
C	2.11482	5.39950	-1.11478
C	0.02038	3.11177	-1.06534
C	-1.00277	2.17849	-1.03834
H	-0.27187	4.12279	-1.33429
N	-0.86018	0.87118	-0.70580
C	-2.08822	0.26725	-0.68134
C	-2.22477	-1.07673	-0.40539
O	-3.74295	-4.33653	0.02874
C	-3.49436	-1.90292	-0.29072
H	-4.09493	-1.61920	0.58257
C	-4.42032	-1.80081	-1.47859
H	2.76843	6.02907	-0.50195
H	1.08108	5.66615	-0.87957
H	2.29210	5.68392	-2.15960
C	5.32201	5.11572	-1.04619
H	5.65868	3.37498	0.04355
H	4.67418	5.73827	-1.65448
H	6.33894	5.46625	-0.90492
H	6.76588	-0.46396	1.42109
H	6.95259	-0.51619	-0.32773
H	7.14631	-1.98889	0.62511
H	6.10476	-3.94576	0.44671
H	4.53662	-4.70793	0.34356
C	5.12058	-4.17100	2.35072
H	5.70535	-3.40519	2.87035
H	5.56694	-5.14481	2.57242
H	4.11317	-4.15568	2.77874
H	0.31999	-5.66599	1.46070
H	0.33483	-5.97591	-0.26931
H	-1.20016	-5.96837	0.60545
O	-5.56021	-1.38903	-1.44867
O	-3.80118	-2.21539	-2.60367
C	-4.60546	-2.15224	-3.78651
H	-3.97572	-2.52622	-4.59157

H	-4.91305	-1.12205	-3.98394
H	-5.49820	-2.77088	-3.67410
C	-2.43120	2.48216	-1.44579
C	-3.20508	1.26344	-0.89192
C	-3.97991	1.52414	0.40736
H	-3.92570	0.89634	-1.63296
H	-2.44398	2.39820	-2.54405
C	-2.96620	3.85896	-1.08870
C	-3.09213	1.77360	1.62454
H	-4.64426	0.67376	0.60355
H	-4.63596	2.39009	0.27122
H	-2.94620	4.05425	-0.01234
H	-4.00281	3.96991	-1.41939
H	-2.38716	4.64506	-1.58160
H	-2.62119	0.84078	1.96136
C	-3.85145	2.45724	2.74283
H	-2.26481	2.44622	1.35698
O	-4.56905	3.43077	2.53438
N	-3.65961	1.92962	3.98590
H	-3.06095	1.12471	4.07924
C	-4.27321	2.48376	5.16956
H	-4.88986	3.32518	4.85219
H	-3.52198	2.84320	5.87995
H	-4.90912	1.74759	5.67045
Zn	1.07780	-0.04071	-0.32103

C

N	-1.96430	2.07873	-0.59148
C	-3.29213	2.32872	-0.45649
C	-3.54654	3.75348	-0.46796
C	-2.32601	4.36451	-0.61674
C	-1.34200	3.30462	-0.68931
C	-4.26830	1.32539	-0.32249
C	-4.88341	4.38915	-0.32974
C	-2.03081	5.82699	-0.64421
C	0.03048	3.47245	-0.83055
C	0.99358	2.45455	-0.90721
H	0.39710	4.49569	-0.88545
N	0.65451	1.09831	-0.88143
C	2.41063	2.61789	-1.01134
C	2.92104	1.31313	-1.05729
C	3.14634	3.90845	-1.08574
C	1.80943	0.43597	-0.98450
C	4.11913	0.52053	-1.04072
C	-4.07830	-0.04850	-0.29473

H	-5.29481	1.67224	-0.23287
N	-2.85355	-0.68000	-0.40720
C	-5.12310	-1.04303	-0.14373
C	-4.51459	-2.27088	-0.16140
C	-3.09634	-2.01954	-0.33762
C	-5.10414	-3.62943	-0.02628
C	-2.12839	-3.02611	-0.43310
C	-0.75833	-2.89680	-0.61739
H	-2.50632	-4.04328	-0.37538
N	-0.08904	-1.72287	-0.70836
C	1.25504	-1.96977	-0.83846
C	2.15626	-0.93264	-0.96968
O	5.29426	0.86709	-0.87579
C	3.67650	-0.97195	-1.11675
H	4.17220	-1.53169	-0.31235
C	4.09199	-1.66755	-2.40105
H	-6.18731	-3.58124	0.07069
H	-4.69329	-4.15451	0.84406
H	-4.88098	-4.24786	-0.90297
H	-5.32073	4.20675	0.65893
H	-5.59681	4.00694	-1.06798
H	-4.82600	5.47249	-0.46114
H	-2.88171	6.36160	-1.08225
H	-1.18487	6.02602	-1.31366
C	-1.73431	6.39863	0.74162
H	-2.58684	6.25831	1.41331
H	-1.51759	7.46909	0.69242
H	-0.87406	5.89985	1.20011
H	3.08170	4.47694	-0.14923
H	2.74088	4.55981	-1.86685
H	4.20233	3.74647	-1.31300
O	4.35383	-2.84904	-2.47548
O	4.07934	-0.82006	-3.43906
C	4.40521	-1.40961	-4.71056
H	4.36289	-0.59440	-5.42911
H	3.68124	-2.18674	-4.96198
H	5.40406	-1.84756	-4.67747
C	0.16608	-4.08019	-0.81357
C	1.56799	-3.44223	-0.69759
C	2.33297	-3.72933	0.60598
H	2.21692	-3.77872	-1.51316
H	0.03338	-4.39361	-1.86018
C	-0.11191	-5.29007	0.06316
C	1.73429	-3.11766	1.89682
H	3.35780	-3.36236	0.46359
H	2.44324	-4.81098	0.72869

H	-0.08541	-5.04074	1.12834
H	0.62003	-6.08181	-0.11816
H	-1.09647	-5.71438	-0.14874
H	0.94820	-2.39109	1.65415
C	2.83677	-2.44340	2.67537
H	1.28935	-3.88468	2.53305
O	3.48692	-2.97717	3.55925
N	3.12737	-1.15865	2.23798
H	2.68536	-0.87882	1.36640
C	4.45065	-0.63552	2.49418
H	4.72545	-0.93819	3.51044
C	4.42277	0.86679	2.31306
H	5.18481	-1.08953	1.81110
Zn	-1.11320	0.21250	-0.66624
C	-6.57254	-0.72917	0.04353
O	-7.36691	-1.67526	-0.64508
H	-6.77267	0.27938	-0.36692
C	-6.96484	-0.71150	1.52464
H	-6.72514	-1.69023	1.96105
N	-8.40334	-0.51936	1.62626
H	-6.36627	0.04034	2.07107
H	-8.24362	-1.60410	-0.22982
C	-8.93738	-0.81699	2.94667
H	-8.63310	0.43893	1.38014
H	-8.78499	-1.87791	3.16533
H	-10.01248	-0.62655	2.96011
H	-8.47185	-0.23635	3.75982
H	3.74768	1.34228	3.03077
H	4.08496	1.12899	1.30727
N	5.77341	1.54875	2.48361
C	6.08616	1.70045	3.93809
C	5.67578	2.89919	1.83950
C	6.88651	0.79098	1.81318
H	5.32628	2.33032	4.40142
H	7.06841	2.16223	4.04149
H	6.09141	0.71612	4.40662
H	7.06933	-0.13316	2.35982
H	7.77841	1.41759	1.84783
H	6.59908	0.59279	0.77796
H	4.81953	3.42783	2.26120
H	5.54458	2.74556	0.76539
H	6.59431	3.45204	2.03934